Quantum chemical study of the nature of the ground state and the pressure-induced spin transition in CaFeO3

Sadoc, Aymeric; de Graaf, Cornelis; Broer, Ria

Published in:
Physical Review. B: Condensed Matter and Materials Physics

DOI:
10.1103/PhysRevB.75.165116

Publication date:
2007

Quantum chemical study of the nature of the ground state and the pressure-induced spin transition in $CaFeO_3$

Aymeric Sadoc,[1] Coen de Graaf,[2] and Ria Broer[1]
[1]*Theoretical Chemistry, Zernike Institute for Advanced Materials, University of Groningen, Nijenborgh 4, 9747 AG Groningen, The Netherlands*
[2]*ICREA, Department of Physical and Inorganic Chemistry, Universitat Rovira i Virgili, Marcel lí Domingo s/n, 43007 Tarragona, Spain*
(Received 12 December 2006; revised manuscript received 16 February 2007; published 25 April 2007)

Ab initio calculations have been performed to clarify the character of the electronic ground state of the high-temperature phase of $CaFeO_3$ at different external pressures. The analysis of the correlated *N*-electron wave function of properly embedded FeO_6 clusters in terms of optimal atomic orbitals clearly establishes the character of the ground state as being dominated by charge transfer configurations. For all pressures, the number of Fe 3*d* electrons is around 5 and iron should be considered as a Fe^{3+} ion. We find an $S=2$ to $S=1$ transition around 25 GPa in the $CaFeO_3$ crystal.

DOI: 10.1103/PhysRevB.75.165116 PACS number(s): 71.10.−w, 71.27.+a, 71.70.Ch, 71.30.+h

I. INTRODUCTION

Perovskite oxides have been the subject of intense research over the past decade because of the wide range of possible magnetic and electrical properties that can potentially be used in applications. Most of the perovskite oxides exhibit charge, orbital, and magnetic ordering.[1] For some transition metal (TM) oxides that are believed to show charge ordering, the ordering of the charges is still not well understood. This points the interest on $CaFeO_3$, which is, following the ionic model, composed of high-valent Fe^{4+} (d^4) Jahn-Teller (JT) active ions but shows, instead of JT distortion, charge disproportionation at low temperature.

Using powder diffraction techniques, the room- and low-temperature crystal structures of $CaFeO_3$ have been determined by Woodward *et al.*[2] and Takeda *et al.*[3] At 300 K the crystal structure is distorted from the ideal perovskite structure by tilting of the octahedra. Below ~290 K, two distinct Fe signals appear and the symmetry is lowered from the P_{bnm} to the $P_{2_1/n}$ space group. In addition to the tilting of the octahedra, the low-temperature structure exhibits two different Fe sites composed of small and large octahedra. Information about the electronic configuration of the Fe ions at the different sites in the low-temperature phase was derived from the ^{57}Fe Mössbauer spectrum.[4] The single line found at high temperature is split when the temperature is lowered, which has been interpreted from the two different isomer shift values as a transition from paramagnetic non-charge-disproportionated phase, containing equivalent Fe^{4+} ions, to a paramagnetic charge-disproportionated (CD) phase containing Fe^{3+} and Fe^{5+} ions ($T_{CD}=298$ K). A second transition from a paramagnetic charge-disproportionated phase (doublet peak) to an antiferromagnetic charge-disproportionated phase (two sextet peaks, $T_{Néel}=115$ K) has also been characterized. Moreover, *in situ* ^{57}Fe Mössbauer spectroscopy and x-ray diffraction under pressure suggested the existence of yet another phase. The two different signals observed for normal and high pressure were interpreted as a pressure-induced high-spin to low-spin transition.[5] More recently, the presence of one specific mode in the Raman spectra determined by Ghosh *et al.*[6] implies that some JT-type distortion is present at room temperature in $CaFeO_3$, indicating the existence of a JT Fe^{4+} (d^4) ionic state along with the non-JT Fe^{3+} state (d^5L^{-1} where L^{-1} denotes a hole on the oxygen ligands).

The $SrFeO_3$ isoelectronic compound has an almost ideal perovskite crystal structure, the Fe-O-Fe angle=180° compared to 155° for $CaFeO_3$. This compound does not show any indication of CD on decreasing the temperature down to 4 K.[7] Only one iron site is observed among all temperature and pressure variations. Bocquet *et al.*[8] concluded from x-ray and uv photoemission spectroscopy that the ground state of $SrFeO_3$ consists of heavily mixed d^4 and d^5L^{-1} states in agreement with more recent x-ray absorption spectroscopy measurements combined with semiempirical cluster calculations[9] that emphasize a ground state containing considerable O 2*p* hole character. Another interesting comparison can be made with $LaMnO_3$, which is also isoelectronic. The Mn^{3+} (d^4) ions show a strong Jahn-Teller distortion at 750 K[10–12] and all metal sites maintain the same effective charge. This different behavior has been interpreted[13] to indicate that manganites prefer JT distortion because of the weaker covalent character of the Mn-O bond compared to the Fe-O bond.

The marked differences between the local density approximation (LDA) and LDA+*U* band structure reveal the importance of electron correlation in the electronic structure of $CaFeO_3$. Moreover, these calculations indicate a strong Fe 3*d*–O 2*p* mixing.[14] In order to treat these electron correlation effects in a rigorous, *ab initio* way and to quantify the importance of the O 2*p* to Fe 3*d* charge transfer effects, we use the embedded cluster approach in combination with state-of-the-art quantum chemical methods. We investigate the character of the ground state at room temperature and normal pressure and also report the evolution of low-lying excited states with increasing pressure. A cluster containing one Fe ion and the nearest six oxygen anions is considered to represent the material. To introduce the effect of the rest of the crystal this ML_6 cluster is embedded in a set of point charges to account for long-range electrostatic interactions, whereas the nearest ions around the cluster are represented by effective one-electron potentials (see Fig. 1).[15,16] Within this material model the electronic structure can be investi-

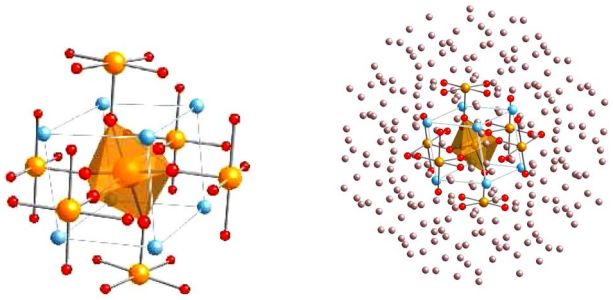

FIG. 1. (Color online) $[FeO_6]^{8-}$ basic cluster embedded in AIEMPs (left) plus the optimized point charges (right).

gated by standard *ab initio* quantum chemical methods. There exist by now a large number of publications in which the embedded cluster model is applied in combination with highly accurate quantum chemical methods to study the electronic structure of transition metal oxides; see, for example, Refs. 17–25, and references therein. Several studies have contrasted cluster calculations with periodic results using the unrestricted Hartree-Fock approach.[26–29]

II. DETAILS OF CALCULATIONS

A. Material model

The electronic structure of an $[FeO_6]$ cluster is represented as accurately as possible with standard quantum chemical procedures as outlined below. The effect of the rest of the crystal is accounted for in the following way. The ions included in a sphere of 5 Å around the central ion (excluding those already in the basic cluster) are represented with *ab initio* embedded model potentials[15] (AIEMPs). This embedding scheme accounts for the finite size of the ions around the cluster and, furthermore, exchange and so-called orthogonality interactions are partially included in the description of the electrostatic structure. The AIEMPs for Ca, Fe, and O in $CaFeO_3$ are optimized following the procedure given in Ref. 30. The implementation of the AIEMPs is based on the theory of electron separability[15,31,32] which assumes a strong orthogonality between the different groups of electrons. For an ideal ionic system the strong orthogonality condition is satisfied and the bare AIEMPs give an accurate representation of the external ions. However, when the cluster wave function has non-negligible amplitude outside the cluster region, the strong orthogonality condition can only be maintained by adding basis functions to the atoms represented by AIEMPs.[33] In the present work we add $(1s, 1p)$ valence basis functions to the oxygen and the iron atoms around the basic cluster (AIEMP-*sp*). In addition, the long-range electrostatic interactions are considered with a set of optimized point charges from the ionic model that reproduce the Madelung field in the cluster region arising from the rest of the crystal. The positions of the atoms in the cluster and its embedding are defined by the crystal structure determination of the room-temperature phase by Woodward *et al.*[2]

B. *N*-electron wave functions

The one-electron basis set employed in the present work to describe the one-electron functions (orbitals) in the cluster region is derived from a $(21s, 15p, 10d, 6f)$ primitive basis set for iron and a $(14s, 9p, 4d)$ primitive basis set for oxygen. Following the atomic natural orbital contraction of Widmark and co-workers,[34,35] we use a $(6s, 5p, 4d, 1f)$ basis for Fe and a $(4s, 3p, 1d)$ basis for O.

The *N*-electron wave function for the state of interest is formed by a linear combination of Slater determinants, the antisymmetric products of the one-electron functions. In the limit of a full configuration interaction (i.e., the consideration of the full list of Slater determinants that can be formed by distributing the electrons in all possible ways over the one-electron functions), this wave function is exact within the given one-electron basis set. This approach is unfortunately only available for very small systems, and hence, we use the complete active space self-consistent field (CASSCF) approach as implemented in the MOLCAS 6.2 code.[36] The expansion of the *N*-electron wave function is constructed by the distribution of a limited number of electrons over a set of valence orbitals, the so-called active space. All other electrons are in doubly occupied orbitals, the so-called inactive orbitals. Two sets of valence orbitals were used. In the first place, we limited the active space to the five orbitals with mainly Fe $3d$ character and a set of virtual orbitals of the same symmetry character. Results referring to this active space will be marked as CAS(4,10). The first number indicates the number of active electrons and the second the number of active orbitals. The second active space extends the first one with two occupied orbitals of e_g-like symmetry with mainly O $2p$ character. The resulting active space is labeled CAS(8,12). This choice of active space ensures a balanced and unbiased treatment of the most important electronic configurations: the non-charge-transfer (NCT) Fe $3d^4$, the charge transfer (CT) Fe $3d^5L^{-1}$, and the double CT (DCT) Fe $3d^6L^{-2}$ configuration.

Since the deviations from a perfect octahedral coordination around the Fe ions are small, the deviations from octahedral level splittings are also small. Thus we will denote for clarity the states by their Russell-Saunders symbols in the case of O_h site symmetry. The eight lowest-lying electronic states were studied: ^5E_g, $^5T_{2g}$, $a\ ^3T_{1g}$, ^3E_g, $b\ ^3T_{1g}$, $^3T_{2g}$, $^1T_{2g}$, and ^1E_g. The excitation energies will be related to the ^5E_g ground state unless stated otherwise. All the calculations were done in the C_i symmetry for the $[FeO_6]^{8-}$ cluster.

Provided that the active space is flexible enough to account for all important nondynamical electron correlation, the CASSCF method gives reasonably accurate electron distributions. However, it fails to reproduce the correct relative energies of the different electronic states due to the lack of dynamical electron correlation effects. These largely atomic effects can efficiently be included in the wave function with complete active space second-order perturbation theory (CASPT2).[37,38] All CASPT2 calculations were done with an imaginary shift of 0.3 hartree to avoid the presence of intruder states.[39] All electrons are correlated except those in the Fe $1s$, $2s$, $2p$, and O $1s$ core orbitals. Both scalar relativistic effects and spin-orbit coupling effects are expected to be small and were not considered in the calculations.

C. Pressure study

The effect of the external pressure is simulated by changing the interatomic distances in the cluster and the embed-

TABLE I. $CaFeO_3$ lattice parameters and average Fe-O distance in Å with increasing pressure. The parameters are deduced from Ref. 2 for 0.1 GPa and Fig. 2 in Ref. 5 for larger pressure.

	0.1 GPa	10 GPa	20 GPa	30 GPa	40 GPa	50 GPa
a	5.31744	5.24673	5.17602	5.09117	5.16195	5.16100
b	5.31744	5.24673	5.17602	5.09117	4.89325	4.83668
c	7.52000	7.42000	7.32000	7.20000	7.20010	7.09000
Fe-O	1.918	1.889	1.865	1.833	1.819	1.803

ding, following closely the changes in lattice parameters reported by Takano and co-workers[5] (see Table I). We evaluate the CASPT2 energies of the excited states relative to the ground state at different pressures using the CAS(8,12) wave function as reference wave function for the perturbational treatment.

III. RESULTS AND DISCUSSION

The two components of the ${}^5E_g$ ground state are almost degenerate in all calculations. The distortion of the octahedral surrounding of the Fe ions is too small to induce a preference for occupying one of the two e_g^* orbitals in the $e_g^4 t_{2g}^{*3} e_g^{*1}$ electronic configuration (see Table II). For clarity the inactive orbitals from a CAS(8,12)SCF are omitted from the notations of the electronic configurations. t_{2g}^* and e_g^* are antibonding linear combinations of Fe 3*d* and O 2*p* basis functions; the e_g orbitals are the bonding counterparts of e_g^*. Figure 2 gives a graphical representation of the orbitals of e_g symmetry and Table III gives a more quantitative account of the character of the orbitals by means of a Mulliken orbital population analysis.

Although the ordering of the different excited states, apart from the ${}^5T_{2g}$ state, is similar in the CAS(4,10) and CAS(8,12) calculations, the effect of extending the active space with the two e_g orbitals of mainly O $2p_\sigma$ character is much more pronounced than in the case of simpler TM oxides like NiO and CoO.[40,41] The total CASSCF energy of the ${}^5E_g$ state is lowered by approximately 2.5 eV by including

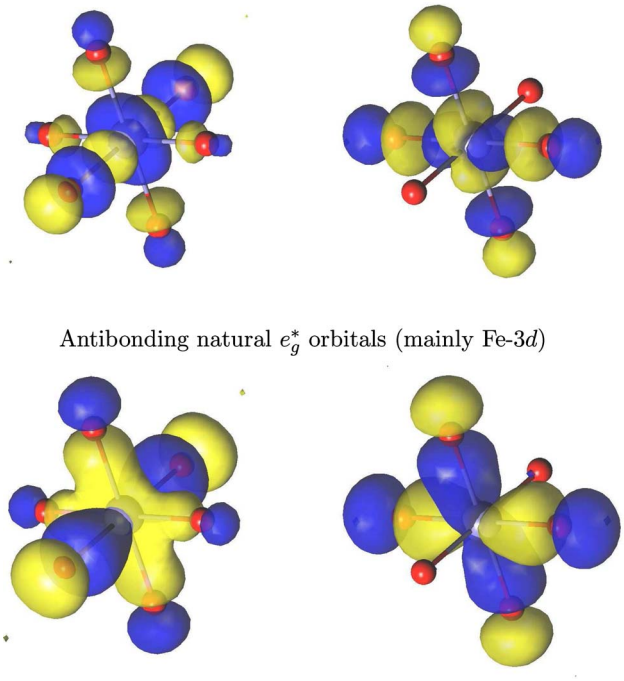

Antibonding natural e_g^* orbitals (mainly Fe-3*d*)

Bonding natural e_g orbitals (mainly O-2*p*)

FIG. 2. (Color online) Bonding and antibonding CAS(8,12) natural e_g-like orbitals for the $[FeO_6]^{8-}$ cluster embedded in AIEMP-*sp* and fitted point charges.

the charge transfer configurations in the active space, whereas a lowering of not more than 0.2 eV was found in the case of NiO. Furthermore, we observe significant changes in the relative energies. All the states with dominant $e_g^4 t_{2g}^{*3} e_g^{*1}$ configurations are stabilized by 2.2–2.5 eV as the ${}^5E_g$ ground state. The states with a dominant $e_g^4 t_{2g}^{*4} e_g^{*0}$ configurations are stabilized by 2.5–3.0 eV. The most striking difference is the rise of the relative energy of the ${}^5T_{2g}$ state from 2.84 to 4.28 eV due to a weaker stabilization by 1.16 eV.

In a simple ionic picture the ${}^5E_g$-${}^5T_{2g}$ energy difference would correspond to the *ab initio* estimate of $10D_q$ in the Racah parametrization scheme. The covalent interactions are,

TABLE II. Relative energies (in eV) of the low-lying electronic states in the embedded FeO_6 cluster to model $CaFeO_3$ at 298 K and ambient pressure. Results are compared at the CAS(4,10)SCF, CAS(8,12)SCF, and the subsequent CASPT2 level calculations. The lattice parameters are taken from Ref. 2.

State	Dominant electronic configuration	CAS(4,10)SCF	CAS(8,12)SCF	CASPT2
${}^5E_g$	$e_g^4\ t_{2g}^{*3}\ e_g^{*1}$	0.00; 0.06	0.00;[a] 0.05	0.00; 0.04
$a\ {}^3T_{1g}$	$e_g^4\ t_{2g}^{*4}\ e_g^{*0}$	0.61; 0.63; 0.68	0.24; 0.27; 0.30	0.46; 0.50; 0.52
${}^1T_{2g}$	$e_g^4\ t_{2g}^{*4}\ e_g^{*0}$	2.23; 2.26; 2.29	2.04; 2.07; 2.11	1.98; 1.99; 2.02
${}^1E_g$	$e_g^4\ t_{2g}^{*4}\ e_g^{*0}$	2.45; 2.48	2.21; 2.24	2.16; 2.19
${}^3E_g$	$e_g^4\ t_{2g}^{*3}\ e_g^{*1}$	2.54; 2.59	2.64; 2.69	2.26; 2.30
$b\ {}^3T_{1g}$	$e_g^4\ t_{2g}^{*3}\ e_g^{*1}$	3.06; 3.09; 3.10	3.42; 3.45; 3.47	2.72; 2.72; 2.74
${}^3T_{2g}$	$e_g^4\ t_{2g}^{*3}\ e_g^{*1}$	3.19; 3.20; 3.23	3.52; 3.54; 3.57	2.82; 2.82; 2.82
${}^5T_{2g}$	$e_g^4\ t_{2g}^{*2}\ e_g^{*2}$	2.84; 2.86; 2.86	4.28; 4.29; 4.32	3.42; 3.43; 3.47

[a]The total energy obtained with CAS(8,12)SCF is 2.59 eV below that obtained with CAS(4,10).

TABLE III. Character of the active orbitals in the CAS(4,10)SCF and CAS(8,12)SCF calculations determined by Mulliken-Gross population analysis.

	CAS(4,10)			CAS(8,12)		
Orbital	Occupation No.	Fe 3*d*	O 2*p*	Occupation No.	Fe 3*d*	O 2*p*
e_g	4.00			3.80	0.33	0.67
t_{2g}^*	3.00	0.96	0.04	3.00	0.97	0.03
e_g^*	1.00	0.74	0.26	1.20	0.67	0.33

however, so strong that the appropriateness of this simple model is questionable and we prefer to speak here about the t_{2g}^*-e_g^* splitting. Table III shows a transfer of about 0.2 electrons from the e_g to the e_g^* orbitals upon the extension of the active space with the e_g orbitals. On the other hand, the occupation of the t_{2g}^* orbitals remains 3.00, indicating that all charge transfer occurs within the orbitals of e_g symmetry. This flow of electrons (de)stabilizes the (anti)bonding orbitals. Since the extension of the active space hardly affects the t_{2g}^* orbitals, the transition from the ${}^5E_g$ state to the ${}^5T_{2g}$ state, in which one electron is transferred from the t_{2g}^* orbital to the e_g^* orbital, becomes energetically less favorable.

The effect of the bonding t_{2g} orbitals with mostly O 2*p* character is smaller. Therefore, we do not treat these excitations in the CASSCF method but their effect is estimated with second-order perturbation theory. Due to symmetry, these excitations have a smaller interaction with the ${}^5E_g$ state than with the ${}^5T_{2g}$ state; the t_{2g}^*-e_g^* splitting is decreased again, giving our final estimate of 3.4 eV. The electron correlation accounted for by CASPT2 increases the splitting of the two lowest states ${}^5E_g$ and *a* ${}^3T_{1g}$ to 0.5 eV.

A. Character of the ground state

The interpretation of the cluster wave function in terms of NCT (Fe $3d^4$) and CT (Fe $3d^5L^{-1}$) determinants is not straightforward since the information on covalency is contained in two different places in the multiconfigurational wave function: first in the orbitals, which have a mixed character with important contributions from the Fe 3*d* and O 2*p* basis functions as can be seen in the population analysis resumed in Table III; second, in the configuration-interaction (CI) expansion of the wave function, where the different electronic configurations (NCT, CT, DCT, etc.) appear with different weights.

Since the choice of the orbitals to express the *N*-electron CASSCF wave function is not unique, it is possible to establish more clearly the importance of charge transfer in this system by performing a transformation of the orbitals. The analysis of Cooper *et al.*[42,43] and the complete active space valence bond approach of Hirao *et al.*[44] involve transformations among all active orbitals, allowing one to interpret the CASSCF wave function in term of valence bond structures. Both approaches lead to an interpretation in terms of nonorthogonal localized orbitals[42,43] or nonorthogonal spin functions.[44] In this study we simply rotate pairs of orbitals in the active space in order to minimize the mixing of Fe 3*d* and O 2*p* basis functions in the orbitals. We make linear combinations of bonding and antibonding orbitals of e_g-like character. This unitary transformation does not affect the energy expectation value of the ground state. Figure 3 shows the obtained atomiclike orbitals after transformation of the natural orbitals. After reexpressing the CI expansion of the wave function in terms of the atomiclike orbitals the information on the covalence is entirely concentrated in the wave function expansion. The length of the CI expansion for the CAS(8,12)SCF quintet wave function is 60 984 determinants. Summing up the squared coefficients of all the determinants with four, three, two, or one electron(s) in the O-centered atomiclike orbitals, the ${}^5E_g$ ground state can be schematically written as

$$18.9\ \%\ \mathrm{NCT} + 66.2\ \%\ \mathrm{CT} + 14.0\ \%\ \mathrm{DCT} + 0.4\ \%\ \mathrm{TCT} + \cdots .$$

This analysis provides theoretical evidence that the ground state is dominated by the Fe $3d^5L^{-1}$ electronic configuration where the five *d* electrons are mainly coupled to ${}^6A_{1g}$. This leading configuration is not Jahn-Teller active, and hence can explain why no JT distortion is observed in $CaFeO_3$ at room temperature and why the material prefers to go through charge disproportionation while maintaining octahedral symmetry. The high formal charge of Fe may also give rise to CT from O $2p_\pi$ orbitals of t_{2g} symmetry. However, because the interaction between Fe $3d(t_{2g})$ and O $2p_\pi$ is quite weak, the

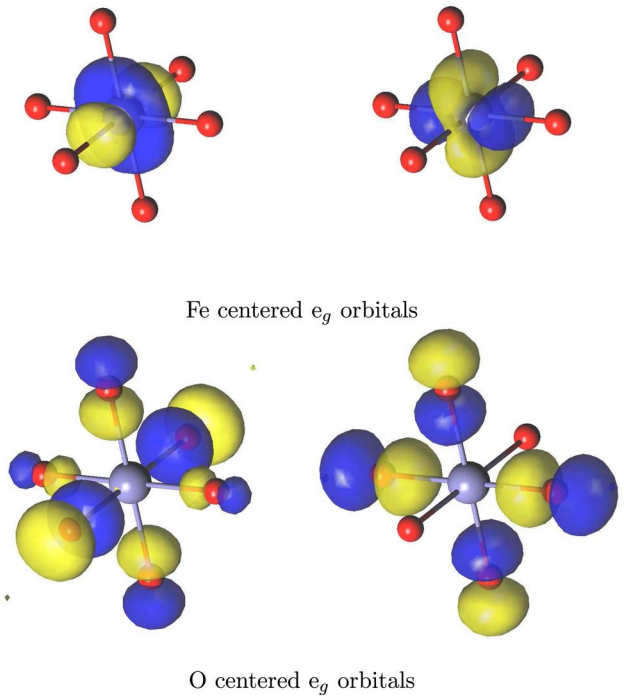

FIG. 3. (Color online) Optimal atomic e_g-like orbitals obtained from a unitary transformation of the CAS(8,12) natural orbitals of the $[FeO_6]^{8-}$ cluster embedded in AIEMP-*sp* and fitted point charges.

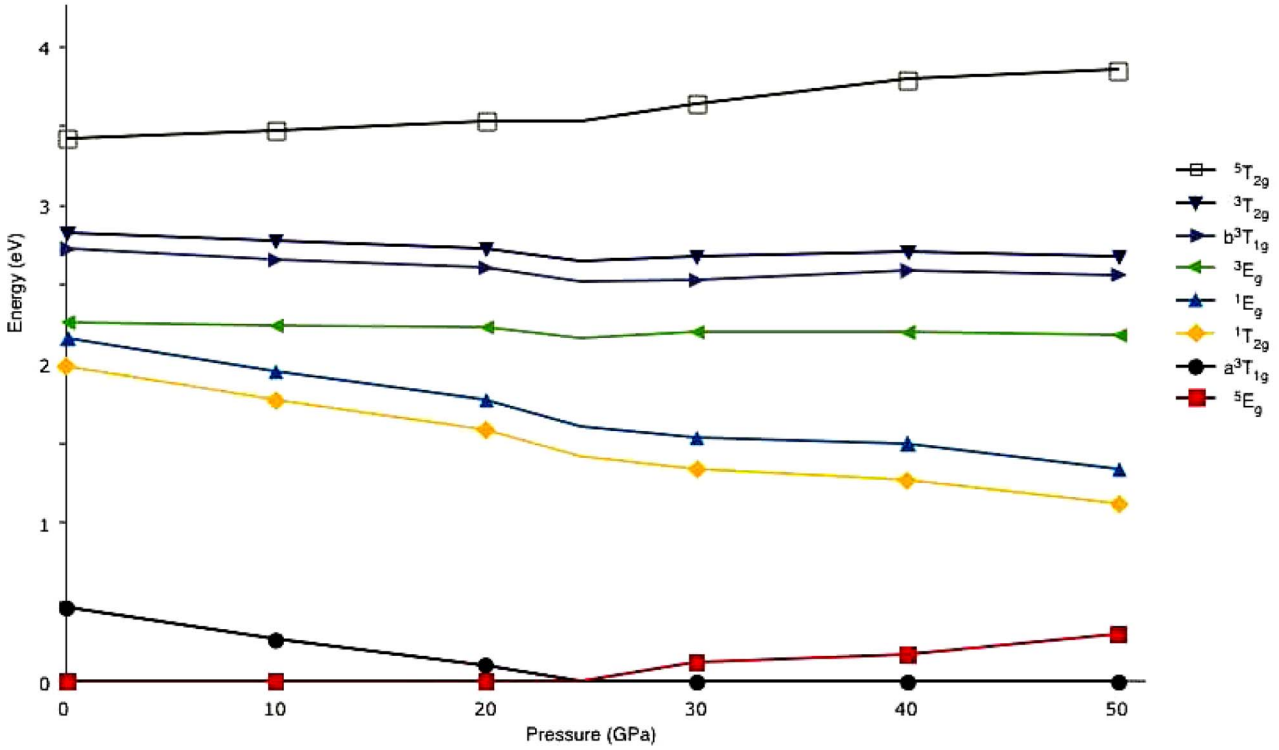

FIG. 4. (Color online) Evolution of the CASPT2 energies with pressure. The lines connecting the markers are a guide to the eyes.

t_{2g} orbitals are already essentially O $2p_\pi$ orbitals and the t_{2g}^* orbitals are already almost pure Fe $3d$ orbitals. A rotation amongst these orbitals would slightly lower the weight of the NCT configuration. Notice that the embedding of the FeO_6 cluster is constructed using Fe^{4+} and O^{2-} ions. This means that the external potential could bias the NCT (Fe $3d^4$–O $2p^6$) configuration. Hence, the weight of 18.9% should be considered as an upper estimate.

The analysis also provides a way to estimate the effective oxidation state (or net charge) of the Fe-ion. The total number of Fe $3d$ electrons x is given by $\Sigma_i \alpha_i \times x_i$. The sum runs over all the different configurations, and α_i and x_i correspond to the weights and the number of d electrons of these configurations. Given that the t_{2g}^* orbitals are atomiclike and occupied with three electrons, we have $x=0.189\times4+0.662\times5+0.140\times6+0.004\times7=4.93$ electrons. Hence, Fe in $CaFeO_3$ is closer to Fe^{3+} than to the formal Fe^{4+}.

B. Influence of pressure

We proceed with the scheme above described by using AIEMPs with s and p functions for the first shell of atoms around our cluster and a set of point charges using the lattice parameters reported by Takano *et al.*[5] Figure 4 shows the evolution of the relative energies at the CASPT2 level of the different states by increasing the pressure. The ground state energy is taken as reference energy.

The CASPT2 energies follow closely the Tanabe-Sugano diagram for a d^4 ion in octahedral symmetry.[45] This shows that the simple ionic model is a useful ansatz to explain the relative energies, provided that all relevant electronic effects are taken into account. In the Tanabe-Sugano diagrams this is accomplished via parametrization of the B/C and $10Dq$ values. In our CASPT2 approach these effects are included via the orbital delocalization and excited configurations. The energies form a smooth curve between 0 and 20 GPa, as can be expected from the gradual reduction of the lattice parameters $a=b$ and c in this pressure range (see Table I). At ≈25 GPa the ligand field is strong enough to induce a spin crossing. The $a\ ^3T_{1g}$ state becomes the ground state of the system. This result is in reasonable agreement with the Mössbauer study realized by Takano *et al.*[5] who measured a pressure-induced spin transition at 30 GPa. The energies at 40 and 50 GPa, where the a and b lattice parameters are no longer equal, do not form a smooth continuation of the energies for lower pressures, but we do see the same trends for increasing pressure.

We also investigate the evolution of the character of the ^5E_g and $a\ ^3T_{1g}$ wave functions with pressure by performing the same unitary transformation on the orbitals as used previously. Table IV shows the weights of the various configurations as a function of pressure. The CT character of the wave function (defined as the sum of the weights of the CT, DCT, and TCT configurations) decreases continuously with increasing pressure for the ^5E_g state up to the phase transition around 30 GPa. This decrease is a consequence of the destabilization of the Fe $3d(e_g)$ orbitals due to increased ligand field. The abrupt change in the structure at the phase transition causes a discontinuity in this tendency but the CT character decreases again from 40 to 50 GPa. Furthermore, we observe a weaker contribution of NCT configurations in the $a\ ^3T_{1g}$ than in the ^5E_g state. As for the ^5E_g state, the charge

TABLE IV. Evolution of the weights in % of the various valence bond configurations and number of Fe d electrons as a function of the pressure (in GPa) for the ^5E_g and $a\ ^3T_{1g}$ states.

Pressure	NCT	CT	DCT	TCT	Fe $3d^x$
		^5E_g			
0.1	18.9	66.2	14.0	0.4	4.93
10	21.1	64.1	13.7	0.4	4.90
20	22.3	62.6	14.0	0.4	4.89
30	23.6	61.0	14.3	0.5	4.89
40	20.5	60.4	18.6	0.9	4.96
50	22.9	60.1	15.8	0.7	4.92
		$a\ ^3T_{1g}$			
0.1	12.7	55.4	28.4	2.0	5.12
10	13.8	54.9	27.6	2.1	5.10
20	14.5	54.5	27.2	2.2	5.09
30	15.3	53.7	27.0	2.4	5.09
40	15.3	53.3	27.3	2.5	5.09
50	13.1	51.1	30.5	3.7	5.17

transfer for the $a\ ^3T_{1g}$ occurs only within the orbitals of e_g symmetry. The occupation of the t_{2g}^* orbitals remains 4.00. The CT character is stronger in the triplet state because the Fe $3d(e_g)$ shell is empty in the NCT configuration, whereas it is occupied with one electron for the quintet state.

IV. SUMMARY AND DISCUSSION

The crystal field model predicts a ^5E_g (Fe $t_{2g}^3e_g^1$) ground state for the $[FeO_6]^{8-}$ octahedron for the high-temperature $CaFeO_3$ crystal structure. Our CAS(4,10)SCF calculations confirm such a ground state with important Fe $3d$–O $2p$ mixing in the e_g shell as in ligand field theory. We find an $e_g^4t_{2g}^{*3}e_g^{*1}$ electronic configuration with 25% O $2p$ contribution to the antibonding e_g^* orbital. Extension of the active space with the bonding e_g orbitals not only introduces CT configurations in the wave function expansion but also enhances the O $2p$–Fe $3d$ mixing from one-quarter to one-third. Both effects lead to a stronger contribution of Fe $3d^5$ configurations. Using this bonding-antibonding orbital set, this increase in the covalency is not easily quantified. However, expressing the wave function in optimal atomiclike orbitals reveals that the leading configuration in the ^5E_g ground state wave function is O $2p(e_g^3)$–Fe $3d(t_{2g}^3e_g^2)$. The number of Fe $3d$ electrons is close to 5, and hence Fe in the high-temperature phase of $CaFeO_3$ has to be considered as an Fe^{3+} ion.

The pressure dependence of the CASPT2 energies of the lowest electronic states leads to a spin transition, as seen in Mössbauer spectroscopy. Between 20 and 30 GPa the ground state changes from ^5E_g to $a\ ^3T_{1g}$. We note that our CASPT2 approach is known to slightly overestimate the energies of high-spin states.[46] Our estimate is that a more accurate account of the electron correlation effects will lower the $a\ ^3T_{1g}$ with respect to the ^5E_g, leading to a spin transition around 20 GPa. In the whole pressure range, the number of Fe $3d$ electrons is around 5. The quintet state is dominated by the CT configuration with important, almost equal, contributions from the NCT and DCT configurations. For the triplet state, the NCT is less important and the DCT becomes twice as important compared to the ^5E_g state.

The present study concerns the high-temperature structure of $CaFeO_3$. Below 290 K the structure is $P2_{1/n}$, containing alternating large and small FeO_6 octahedra. Charge disproportionation is assumed, but there is no generally accepted picture of the electronic structure. The geometry of the small octahedron is close to that of 20 GPa. We find for this geometry that the high-spin ^5E_g and low-spin $a\ ^3T_{1g}$ states are very close in energy. It is possible that the ground state of the low-temperature phase is ferrimagnetic with alternating $S=2$ and $S=1$ octahedra. A more detailed study of the low-temperature phase electronic structure is subject of current investigation.

ACKNOWLEDGMENTS

We thank Ibério de P. R. Moreira for useful discussions. Financial support has been provided by the Spanish Ministry of Education and Science under Project No. CTQU2005-08459-C02-02/BQU, and the Generalitat de Catalunya (Grant No. 2005SGR-00104). Grants for computing time, awarded by the Stichting Nationale Computerfaciliteiten (NCF), contributed to the results reported in this paper.

[1] P. G. Radaelli, D. E. Cox, M. Marezio, and S.-W. Cheong, Phys. Rev. B **55**, 3015 (1997).
[2] P. M. Woodward, D. E. Cox, E. Moshopoulou, A. W. Sleight, and S. Morimoto, Phys. Rev. B **62**, 844 (2000).
[3] T. Takeda, R. Kanno, Y. Kawamoto, M. Takano, S. Kawasaki, T. Kamiyama, and F. Izumi, Solid State Sci. **2**, 673 (2000).
[4] S. Nasu, T. Abe, K. Yamamoto, S. Endo, M. Takano, and Y. Takeda, Hyperfine Interact. **70**, 1063 (1992).
[5] M. Takano, S. Nasu, T. Abe, K. Yamamoto, S. Endo, Y. Takeda, and J. B. Goodenough, Phys. Rev. Lett. **67**, 3267 (1991).
[6] S. Ghosh, N. Kamaraju, M. Seto, A. Fujimori, Y. Takeda, S. Ishiwata, S. Kawasaki, M. Azuma, M. Takano, and A. K. Sood, Phys. Rev. B **71**, 245110 (2005).
[7] S. Nasu, T. Kawakami, S. Kawasaki, and M. Takano, Hyperfine Interact. **144-145**, 119 (2002).
[8] A. E. Bocquet, A. Fujimori, T. Mizokawa, T. Saitoh, H. Namatame, S. Suga, N. Kimizuka, Y. Takeda, and M. Takano, Phys. Rev. B **45**, 1561 (1992).
[9] M. Abbate, G. Zampieri, J. Okamoto, A. Fujimori, S. Kawasaki, and M. Takano, Phys. Rev. B **65**, 165120 (2002).
[10] E. O. Wollan and W. C. Koehler, Phys. Rev. **100**, 545 (1955).
[11] J. B. Goodenough, Phys. Rev. **100**, 564 (1955).

[12] J. Rodríguez-Carvajal, M. Hennion, F. Moussa, A. H. Moudden, L. Pinsard, and A. Revcolevschi, Phys. Rev. B **57**, R3189 (1998).
[13] M.-H. Whangbo, H.-J. Koo, A. Villesuzanne, and M. Pouchard, Inorg. Chem. **41**, 1920 (2002).
[14] T. Saha-Dasgupta, Z. S. Popović, and S. Satpathy, Phys. Rev. B **72**, 045143 (2005).
[15] Z. Barandiarán and L. Seijo, J. Chem. Phys. **89**, 5739 (1988).
[16] C. de Graaf, C. Sousa, and R. Broer, J. Mol. Struct.: THEOCHEM **458**, 53 (1999).
[17] G. J. M. Janssen and W. C. Nieuwpoort, Phys. Rev. B **38**, 3449 (1988).
[18] R. L. Martin, J. Chem. Phys. **98**, 8691 (1993).
[19] D. Muñoz, F. Illas, and I. de P. R. Moreira, Phys. Rev. Lett. **84**, 1579 (2000).
[20] A. Klimkāns and S. Larsson, J. Chem. Phys. **115**, 466 (2001).
[21] L. Hozoi, A. H. de Vries, and R. Broer, Phys. Rev. B **64**, 165104 (2001).
[22] C. J. Calzado and J.-P. Malrieu, Phys. Rev. B **63**, 214520 (2001).
[23] M. B. Lepetit, N. Suaud, A. Gellé, and V. Robert, J. Chem. Phys. **118**, 3966 (2003).
[24] C. J. Calzado, C. de Graaf, E. Bordas, R. Caballol, and J.-P. Malrieu, Phys. Rev. B **67**, 132409 (2003).
[25] E. Bordas, C. de Graaf, R. Caballol, and C. J. Calzado, Phys. Rev. B **71**, 045108 (2005).
[26] J. M. Ricart, R. Dovesi, C. Roetti, and V. R. Saunders, Phys. Rev. B **52**, 2381 (1995).
[27] I. de P. R. Moreira and F. Illas, Phys. Rev. B **55**, 4129 (1997).
[28] Y.-S. Su, T. A. Kaplan, S. D. Mahanti, and J. F. Harrison, Phys. Rev. B **59**, 10521 (1999).
[29] D. Muñoz, I. de P. R. Moreira, and F. Illas, Phys. Rev. B **71**, 172505 (2005).
[30] L. Seijo and Z. Barandiarán, J. Chem. Phys. **94**, 8158 (1991).
[31] S. Huzinaga and A. A. Cantu, J. Chem. Phys. **55**, 5543 (1971).
[32] R. McWeeny, Proc. R. Soc. London, Ser. A **253**, 242 (1959).
[33] J. L. Pascual, L. Seijo, and Z. Barandiarán, J. Chem. Phys. **98**, 9715 (1993).
[34] P.-O. Widmark, P.-Å. Malmqvist, and B. O. Roos, Theor. Chim. Acta **77**, 291 (1990).
[35] R. Pou-Amérigo, M. Merchán, I. Nebot-Gil, P.-O. Widmark, and B. O. Roos, Theor. Chim. Acta **92**, 149 (1995).
[36] G. Karlström *et al.*, Comput. Mater. Sci. **28**, 222 (2003).
[37] K. Andersson, P.-Å. Malmqvist, B. O. Roos, A. J. Sadlej, and K. Wolinski, J. Chem. Phys. **94**, 5483 (1990).
[38] K. Andersson, P.-Å. Malmqvist, and B. O. Roos, J. Chem. Phys. **96**, 1218 (1992).
[39] N. Forsberg and P.-Å. Malmqvist, Chem. Phys. Lett. **274**, 196 (1997).
[40] C. de Graaf, R. Broer, and W. C. Nieuwpoort, Chem. Phys. **208**, 35 (1996).
[41] C. de Graaf, W. A. de Jong, R. Broer, and W. C. Nieuwpoort, Chem. Phys. **237**, 59 (1998).
[42] T. Thorsteinsson, D. L. Cooper, J. Gerratt, P. B. Karadakov, and M. Raimondi, Theor. Chim. Acta **93**, 343 (1996).
[43] T. Thorsteinsson and D. L. Cooper, Int. J. Quantum Chem. **70**, 637 (1998).
[44] K. Hirao, H. Nakano, K. Nakayma, and M. Dupuis, J. Chem. Phys. **105**, 9227 (1996).
[45] Y. Tanabe and C. S. Sugano, J. Phys. Soc. Jpn. **9**, 753 (1954).
[46] G. Ghigo, B. Roos, and P.-Å. Malmqvist, Chem. Phys. Lett. **396**, 142 (2004).